Journal of Gynecological Oncology

Research Article
Published: 30 May, 2024

HER-2 and TME Dual Targeting Shikonin-Loaded Nanomicelle for Anti-Breast Cancer Treatment

Huang RC[1,4#], Luo YJ[1#], Su YH[2,3] and Ling CQ[1]**

[1]Naval Medical University (Second Military Medical, University), China

[2]Department of Dermatology, Yueyang Hospital of Integrated Traditional Chinese and Western Medicine, Shanghai University of Traditional Chinese Medicine, China

[3]Institute of Dermatology, Shanghai Academy of Traditional Chinese Medicine, China

[4]Department of Outpatient, Hangu Traditional Chinese Medicine Hospital in Binhai New Area, China

[#]These authors contributed equally to this work

Abstract

Objectives: Several Chinese traditional medicines have been used in chemotherapy, with Shikonin receiving significant attention for its effective anti-tumor properties. However, its low solubility and lack of precise targeting *in vivo* have limited its biological efficacy, hindering its clinical application. This study focuses on the preparation of Shikonin-loaded Dual targeting Nanomicelles (SDN) that leverage antibody-antigen interactions and tumor microenvironment responsiveness. The anti-Human Epidermal growth factor Receptor-2 antibodies (anti-Her-2) attached to the surface of SDN can effectively target Her-2, a protein that is overexpressed in SKBr-3 cells and BT-474 cells. On the other hand, in response to a slightly higher temperature in tumor tissue, SDN can undergo a phase transition, potentially facilitating endocytosis due to increased hydrophobicity. In this study, we investigate the anti-tumor effects of SDN on *in vitro* and *in vivo* breast cancer models with high expression of her-2 positive.

Methods: To enhance targeted delivery of shikonin to tumor sites, we developed a Nanodrug Delivery System (SDN), characterized it, and used it to treat BT-474 and SKBR-3 cell lines. Cell proliferation was observed through CCK8 experiments. Acute toxicity experiments involved tail vein injections to assess the potential toxic and side effects of SDN on mouse organs, evaluating its safety. The anti-tumor efficacy of SDN was validated using a BT-474 mouse subcutaneous tumor model.

Results: SDN exhibited a complete core-shell spherical shape with excellent serum stability. It demonstrated significant inhibition of HER-2-positive cell proliferation. Acute toxicity experiments indicated improved safety of SDN with reduced organ damage. *In vivo* tumor inhibition experiments revealed that SDN outperformed traditional shikonin in tumor suppression.

Conclusion: By developing Shikonin-loaded Dual targeting Nanomicelles (SDN), this study addressed the limitations of traditional shikonin such as poor water solubility and low targeting efficiency. The enhanced anti-tumor efficacy and biosafety of shikonin warrant further investigation.

Keywords: Shikonin; Nanomicelle; Dual-targeting; Anti-tumor; Safety

OPEN ACCESS

Correspondence:
Yong-Hua Su, Department of Dermatology, Yueyang Hospital of Integrated Traditional Chinese and Western Medicine, Shanghai University of Traditional Chinese Medicine, China, Chang-Quan Ling, Naval Medical University (Second Military Medical, University), 200433, Shanghai, China,

Received Date: *29 Apr 2024*
Accepted Date: *22 May 2024*
Published Date: *30 May 2024*

Citation:
Huang RC, Luo YJ, Su YH, Ling CQ. HER-2 and TME Dual Targeting Shikonin-Loaded Nanomicelle for Anti-Breast Cancer Treatment. J Gynecol Oncol. 2024; 6(1): 1081.

Introduction

Breast cancer is a prevalent form of malignant tumors among women worldwide [1,2], ranking as the sixth leading cause of female cancer-related deaths in China [3]. Surgery is typically the primary treatment in the early stages of breast cancer, often accompanied by adjuvant therapies. In advanced stages, chemotherapy or radiotherapy are commonly utilized; however, these treatments may yield unsatisfactory outcomes in certain cases [4-7].

Shikonin, a natural naphthalene compound isolated from traditional Chinese medicine, has been found to possess anti-cancer, antiviral, and anti-inflammatory properties [8]. Since the publication of the first research report by Hashimoto et al. [9], there has been a growing interest in utilizing Shikonin for cancer treatment. Recent studies have investigated the anti-tumor effect of Shikonin on various tumor models [10-13], providing valuable insights into its mechanism of action.

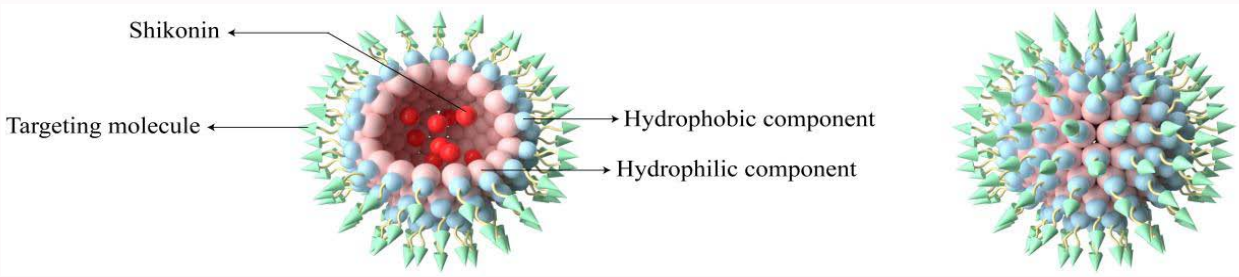

Figure 1: Schematic illustration of SDN model.

Shikonin has demonstrated significant effectiveness in inhibiting the growth and metastasis of breast cancer [10], successfully prolonged animal survival time and reduced tumor size by using Shikonin in combination with paclitaxel [11], illustrated that Shikonin suppressed the proliferation of MCF-7 breast cancer cells by reducing the expression of tumor-promoting miR-128. Thakur et al. [12] discovered that Shikonin hindered breast cancer growth by decreasing the activity of STAT3, FAK, and SRC [13], demonstrated that Shikonin could enhance the immunogenicity of breast tumor cells through direct binding with nuclear protein A1. Despite its promising effects, the limited solubility and inadequate targeting *in vivo* have hindered its clinical application [14,15]. By utilizing a smart Drug Delivery System (DDS) may offer a solution to overcome the two obstacles.

Nanomicelles, composed of amphiphilic block copolymers, are a common Drug Delivery System (DDS) [16-19]. By considering the distinct tumor microenvironment characterized by higher temperature and lower pH, smart DDS with various stimulus responsiveness can be developed to selectively target tumor tissue. Additionally, by enhancing passive targeting, specific antibodies can be attached to the DDS to combine active and passive targeting, effectively minimizing the side effects of chemotherapy [20-23]. So, degradable polymers were synthesized to prepare temperature-sensitive nanomicelles with Shikonin embedded in the core. The decreased integrity of capillary endothelium at the tumor site results in larger cell gaps compared to normal tissue, allowing nanocarriers (100-600 nm) to penetrate through and exploit the enhanced permeability and retention effect (EPR effect) [24-26]. Furthermore, the restricted lymphatic reflux due to loss of lymphatic vessels facilitates accumulation at the tumor site [27-29]. Additionally, the nanomicelles can undergo a phase transition in response to slightly higher temperatures, increasing hydrophobicity and promoting endocytosis. Experimental results demonstrate a significant increase in cytotoxicity of the drug-loaded nanomicelles towards MCF-7 cells [30].

This study aimed to synthesize SDN with dual characteristics of temperature sensitivity and antibody targeting, and investigate its anti-cancer effects on breast cancer models through *in vitro* and *in vivo* experiments. Additionally, the study aimed to compare the toxic and side effects of SDN and traditional monomeric shikonin on animal tissues (Figure 1, 2).

Materials and Methods

Cell lines and materials

Human breast cancer cell lines (SKBR3, BT474) with high expression of Her-2 receptor were obtained from the Cell Bank of the Chinese Academy of Sciences in Shanghai. The cells were cultured in DMED supplemented with 10% fetal calf serum and incubated in 5% CO_2 at 37°C. Monomeric shikonin was purchased from Selleck company and resuspended in Dimethyl Sulfoxide (DMSO).

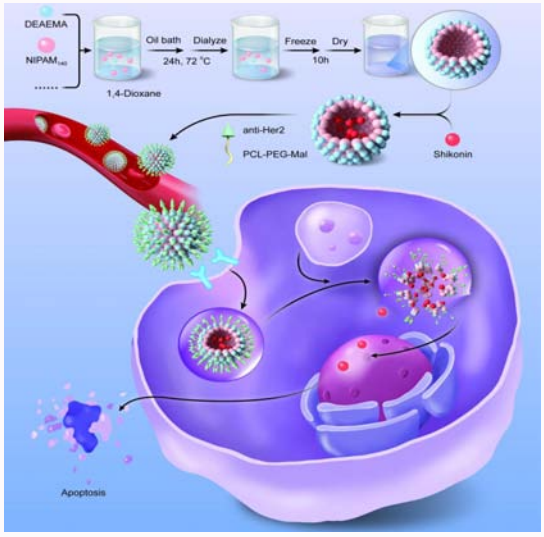

Figure 2: Schematic illustration of SDN targeting and entering cells.

Preparation of FZ-PLGA-NPs

PNIPAM-block-PDPA-co-PDEAEMA copolymers were synthesized using PNIPAM140 as the macro-CTA. A solution containing PNIPAM (10 mM), V501 (2 mM), DPA (1.4 M), and DEAEMA (0.7 M) in 5 mL 1,4-dioxane was degassed through freeze-pump-thaw cycles three times. The polymerization took place in a pre-heated 75°C oil bath for 24 h. Following polymerization, the reaction mixture was cooled in an ice bath and then purified by dialysis against Milli-Q water using a membrane with a MWCO of 1,000 at room temperature for 18 h with regular water changes. The pure block copolymer (PNIPAM140-PDPA70-PDEA70) was obtained after lyophilization for 10 h. To prepare the Shikonin-DMAC solution, 1 ml of 99.0% $C_{16}H_{16}O_5$ (Lot: M1218AS) was added to 1 ml of DMAC solution to achieve a concentration of 1 mg/ml. Subsequently, 3 mg of NiPAM140-PDPA70-PDEA70 was added to 1.5 ml DMAC solution, resulting in a 2 mg/ml polymer-DMAC solution. A mixture of 300 µl of 1 mg/ml Shikonin-DMAC solution with 600 µl of 2 mg/ml polymer-DMAC solution was prepared, incubated for 2 h while protected from light, allowed to stand for 1 h and 30 min, and then dialyzed using a 1 kD membrane for 12 h. By following the aforementioned steps, blank polymer micelles and PCL-PEG-MAL drug-loaded polymer micelles were successfully prepared. 1 mg of BSA was added to 1 ml of PBS (pH=8), which already contained a 1

mg/ml BSA solution. Subsequently, 2.5 mg of 2-IT was added to 0.5 ml of PBS (pH=7), which was mixed with a 5 mg/ml 2-IT solution under light-protected conditions. Under a nitrogen atmosphere, a reaction mixture consisting of 1 ml of 1 mg/ml BSA solution, 50 μl of 100 mM EDTA, and 50 μl of 5 mg/ml 2-IT solution was incubated for 2 h while being shielded from light. To prepare a dialysate, 100 ml of 20 × PBS, 100 ml of 20 × 100 mM EDTA, and 1,800 ml of double-distilled water were combined to yield a final 5 mM EDTA PBS solution. The mercaptogenization of BSA was achieved by dialyzing in a 1 kD membrane for 30 min within the dialysate. The resulting PCL-PEG-MAL drug polymer micelles, along with thiocyanate BSA, were mixed in specific proportions and volumes for 12 h, followed by dialysis using a 30 kD membrane in double-distilled water to obtain polymer micelles attached to BSA. Furthermore, 50 μl of antibody was mixed with 950 μl of PBS at pH=8 to obtain a 1 mg/ml antibody solution, leading to the subsequent formation of SDN (Figures S1-S4).

A 0.25 M Tris-HCl buffer with a pH of 8.3 was prepared using dual vapor. A solution containing 12.116 mg of L-Cys (with a molecular weight of 121.16) was combined with 1 ml of formic acid, and then subjected to double vapor deposition to obtain a final volume of 100 mL, resulting in a 1 mM L-Cys standard solution. Additionally, 198.175 mg of DTNB (with a molecular weight of 396.35) was mixed with 50 ml of 50 mM Na_2HPO_4 buffer (pH=7.0) to create a 10 mM DTNB storage solution, which was shielded from light. The 10 mM DTNB storage solution was then diluted with 0.25 mM Tris-HCl at a ratio of 1:99 to produce a 0.1 mM DTNB analysis solution, which was also protected from light. Prior to analysis, a UV spectrophotometer was preheated for 30 min. Subsequently, 100 μl of 0.25 mM Tris-HCl was placed in a 1.5 ml EP tube for zeroing and as a spare. Following the mixing procedure outlined in Table 1, 100 μl of the solution from the 1.5 ml EP tube was transferred to a new tube. This was followed by adding 50 μl of mercaptogenized BSA to 50 μl of 0.25 M Tris-HCl, and 50 μl of mercaptogenic antibody to another 50 μl of 0.25 M Tris-HCl. In the four EP tubes prepared, 500 μl of the DTNB analysis solution was added, mixed thoroughly, and allowed to stand for 10 min. The spectrophotometer was then set to a wavelength of 412 nm, and a cuvette was prepared for analysis.

One (1) mg of Shikonin was added to 1 ml of acetonitrile to prepare a 1 mg/ml Shikonin-acetonitrile solution. Eight different concentrations of the Shikonin-acetonitrile solution were formulated as per Table 1, 2. The UV spectrophotometer was preheated for 30 min and set to a wavelength of 516 nm. The OD value of the various concentrations of the Shikonin-acetonitrile solution was determined, with each concentration being measured twice and the average taken. In OriginPro 7.0, the OD values were set against the concentration of puricain in the Shikonin-acetonitrile solution as the horizontal coordinate. Subsequently, a standard curve for the absorbance of Shikonin larin synthesis was generated.

Cell proliferation assay

Cells were seeded in the culture medium of a 96-well plate at a density of 4 × 10 cells/well. After 24 h, the cells were exposed to free shikonin, temperature-sensitive nanomicelle-encapsulated shikonin (unlinked HER-2 antibody, single-targeting, referred to as +BSA), and SDN. Treatments were applied at 24, 48, and 72-h time points. Cell viability was assessed using Cell Counting Kit-8, and absorbance was measured at 480 nm using an enzyme-linked immunosorbent assay instrument after 4 h of additional incubation and gentle plate shaking.

Table 1: BSA mercaptogenization efficiency determination.

Solution	EP tube				
	1	2	3	4	5
L-Cy concentration/mM	0.03	0.1	0.1	0.2	0.2
L-Cys standard liquid/μl	12.5	25	50	75	100
Tris-HCl/μl	488	475	450	425	400

Table 2: Determination of shikonin standard curve.

Solution	EP tube							
	1	2	3	4	5	6	7	8
Original dose (μl)	100	80	60	40	20	10	5	2
Acetonitrile (μl)	900	920	940	960	980	990	995	998
Shikonin (μg/ml)	100	80	60	40	20	10	5	2

Acute toxicity test

Healthy BALB/C mice were randomly divided into four groups, each containing 10 mice (Half and half male and female). Following preliminary experiments, the LD50 of monomeric shikonin was successfully determined to be 5.384 mg/kg. To assess the impact of nanomaterials encapsulating shikonin on drug safety, the experiment was divided into four groups: Control group, monomer shikonin group, SDN (low dose), and SDN (high dose). The mice in each group were administered tail vein injections of normal saline, 5.5 mg/kg, and 9 mg/kg of shikonin, respectively. The concentrations were calculated based on the actual shikonin content. Subsequently, the mice were monitored for signs of poisoning and mortality within 24 h, while the main organs of the rats were examined for pathological changes using, HE staining.

Subcutaneous tumor model and immunohistochemical staining

Female BALB/c nude mice aged 6 weeks were obtained from Shanghai Jikai Biotechnology Co., Ltd. The experiment was conducted with four groups, each consisting of five mice (n=5): a control group, a monomeric shikonin group, a +BSA group, and an SDN group. Shikonin was administered at a dosage concentration of 2 mg/kg. BT-474 cells (2×10^6 cells/0.2 mL) were resuspended in PBS solution, then injected subcutaneously into the left hind limb of the nude mice. Drug treatment began when the subcutaneous tumor mass was palpable, administered through tail vein injection. After 15 days of continuous treatment, the mice were euthanized, and the tumors were excised and weighed. Tumor tissues were fixed in formalin, embedded in paraffin, and 5 μm thick tissue sections were prepared for ki-67 immunohistochemical analysis.

Statistical analysis

The significance of the data was assessed using a one-way ANOVA test, and statistical analysis was conducted using IBM SPSS Statistics 27.0 software. A p-value of less than 0.05 was considered statistically significant.

Results

PNIPAM-block-PDPA-Co-PDEAEMA was synthesized using NIPAM as the temperature-sensitive agent, DEAEMA as the synthetic monomer, and V-501 as the initiator, resulting in the production of a pure block copolymer (PNIPAM140-PDPA70-PDEA70). The micelle was self-contained through dialysis technology, with the

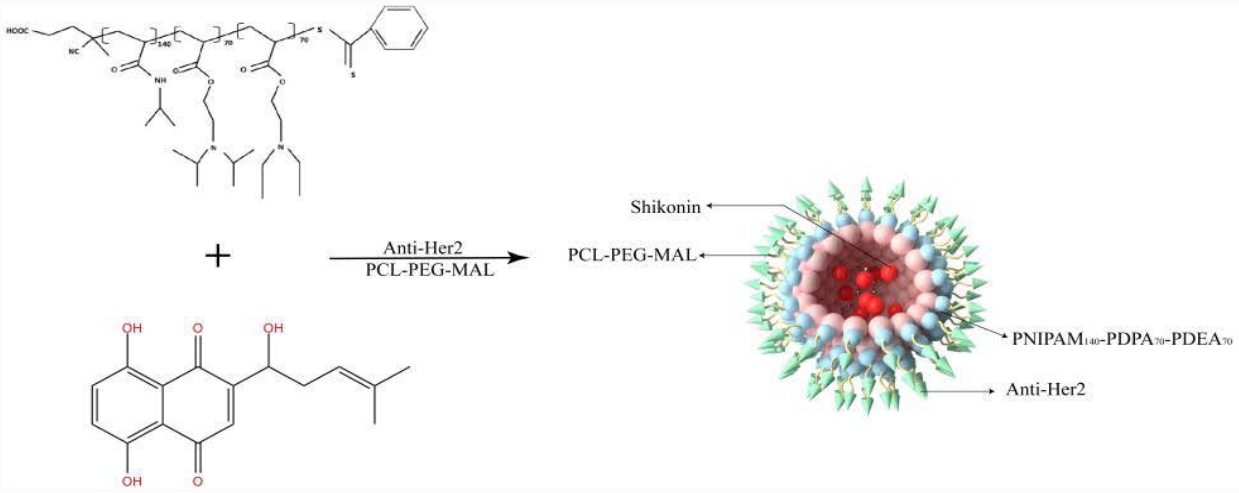

Figure 3: Preparation of SDN.

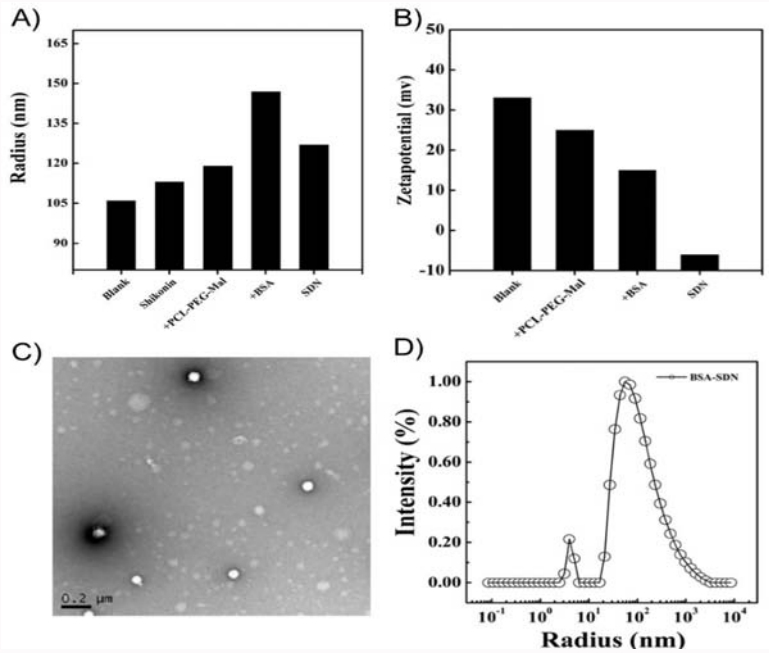

Figure 4: Size A) and zeta potential B) of the nanomicelles with different treatments; C) TEM images of SDN; D) Size of SDN after co-culturing with BSA.

HER-2 antibody covalently attached to its surface, forming a dual targeting SDN encapsulated in a wobble-mein structure, as illustrated in Figure 3. The absorption value of BSA mercaptol after mercapto-glyphylation was determined to be 0.1715. By averaging this value and applying it to the linear formula, the concentration of sulfhydryl groups was found to be 0.102 mg/ml due to dilution. Given that the concentration of BSA is 1 mg/ml with a molecular weight of 68 kDa, the number of sulfhydryl groups per protein molecule was calculated to be 6.94. Similarly, the absorbance value of antibody sulfhydryl was measured to be 0.3505, leading to a thioglyphylation count of 33.39 per antibody molecule, as depicted in Figure S1.

Morphology of SDN

As depicted in Figure 4, the spherical SDN exhibited particle sizes of approximately 50 nm and 200 NMLS, as observed in electron microscope images. Utilizing dynamic light scattering, the polymer particles were measured to be 119 nm, showcasing a core-shell structure in a complete spherical form. Upon loading Shikonin and integrating PEG-b-PCL, BSA, or antibodies, the nanomicelles' sizes increased from 106 nm to 113 nm, 119 nm, 147 nm, and 127 nm, respectively. Post dialysis, the blank micelles in Figure 4 displayed a zeta potential of 33 mV, which decreased to 25 mV upon incorporation of PCL-PEG-mal, and further to 15 mV and -6 mV with the addition of BSA and antibodies, respectively. These alterations in size and zeta potential collectively indicate the successful modification of the

Table 3: Mice treatment groups and number of deaths in acute toxicity experiments.

Solution	Overall	Male deaths	Female deaths	Mortality rate
saline	10	0	0	0%
Shikonin (5.5 mg/kg)	10	2	4	60%
SDN(L) (5.5 mg/kg)	10	1	0	10%
SDN (H) (9 mg/kg)	10	1	1	20%

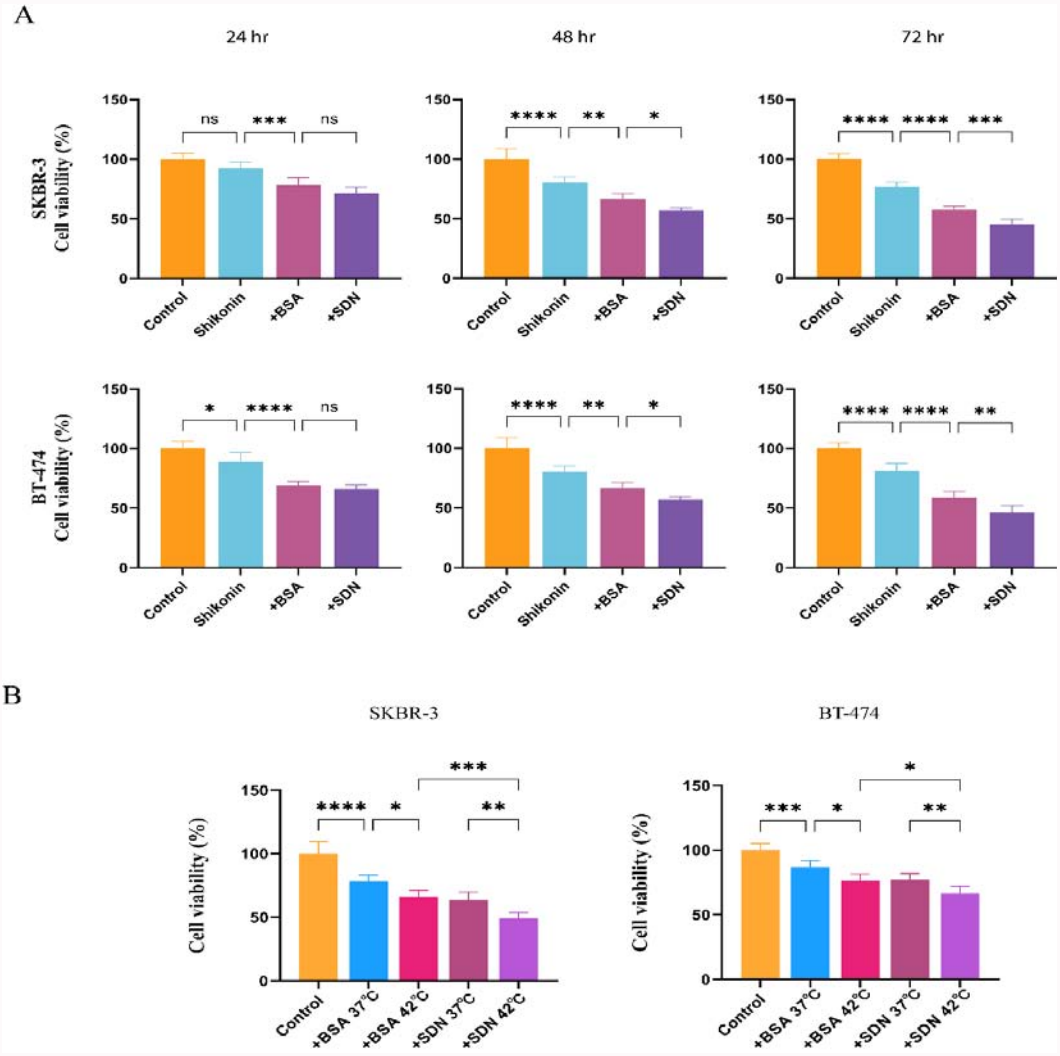

Figure 5: A) Cytotoxicity of nanomicelles towards Skbr-3 and BT-474 cells; B) Cytotoxicity of SDN towards Skbr-3 cells and BT-474 cells at different temperatures; The data in the histogram are mean ± standard deviation; * denotes P<0.05, ** denotes P<0.01, *** denotes P<0.001, NS P>0.05.

nanomicelles. BSA served as a model for serum proteins in circulation within the body. Figure 4 illustrates that when the SDN beam is mixed with BSA, two distinct peaks emerge, consistent with their individual diameters in separate solutions (Figure S5), affirming the stability of SDN and BSA post co-mixing.

EC and EE of SDN

The Shikonin-polymer solution consisted of 2.2 ml with a Shikonin concentration of 136.36 μg/ml and a polymer concentration of 545.45 μg/ml. The blank carrier had a volume of 2.45 ml and a concentration of 734.69 μg/ml. The OD value was measured at 0.08745 and entered into the standard curve equation, resulting in a Shikonin concentration of 6.26 μg/ml. Considering dilution, the calculated Shikonin concentration of SDN was 125.15 μg/ml. The drug delivery efficiency was calculated as 22.94% using the formula (125.15 μg/ml × 2.2 ml)/(0.6 ml × 2 mg/ml). The encapsulation rate, EE, was determined as 91.78% using the formula (125.15 μg/ml × 2.2 ml)/(300 μl × 1 mg/ml) × 100%.

Drug release behavior of SDN

As shown in Figure S6, the release of SDN *in vitro* at 42°C was relatively slow compared to 37°C, with the overall release rate being higher. It was noted that both temperatures resulted in approximately 80% release at 80 h, reaching a stable state by 100 h.

Targeting ability of SDN

At the same temperature, the endocytosis of the SDN group was greater than that of the BSA group, suggesting that the presence of antibodies significantly increased the enrichment of the micelle surface (Figure S7).

Cytotoxicity of SDN *in vitro*

When the concentration of shikonin is below 10 ug/ml, cell toxicity increases as the shikonin concentration rises, as depicted in Figure S8A. The half inhibitory concentration in Figure S8B reveals that the half inhibitory concentration of shikonin is 5.4 μg/ml. Figure 5A illustrates that following treatment with monomeric shikonin, +BSA, and SDN, cytotoxicity towards skbr-3 and bt-474 escalates over time. Concurrently, distinctions in cytotoxicity between +BSA and SDN gradually surface, with statistical analysis demonstrating a significant variance in toxicity between the BSA group and the SDN group after 24 and 48 h of treatment (P<0.05). Furthermore, the outcomes in Figure S9 suggest that SDN exhibits a more potent killing effect on cells with high HER-2 expression compared to HER-2-negative cells.

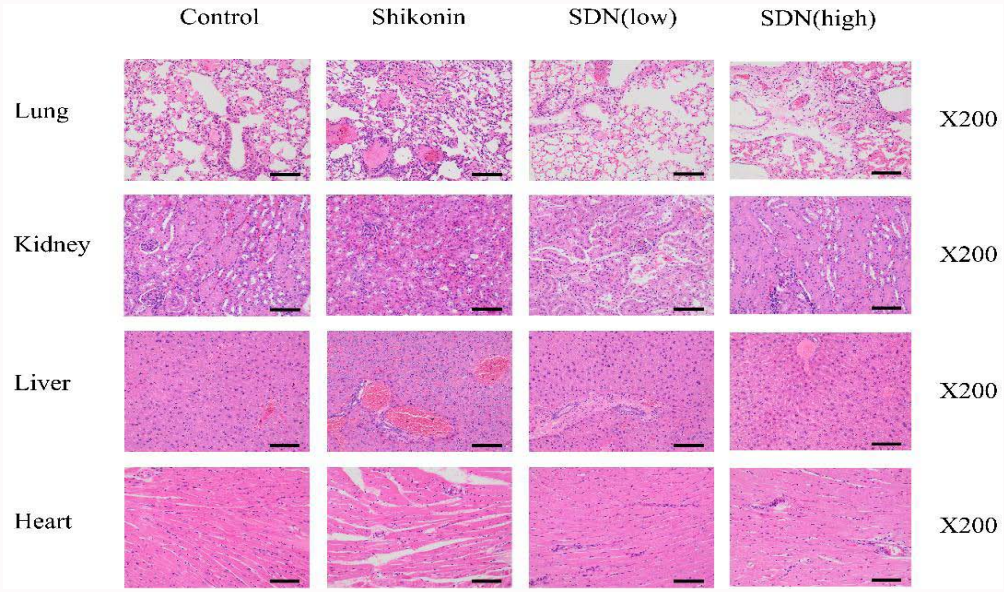

Figure 6: The degree of damage to different organs caused by monomeric shikonin and SDN.

Additionally, in Figure 5B, the temperature sensitivity of the polymer is evident from the contrast in killing effects of BSA-linked micelles (+BSA) and SDN at 37°C and 42°C ($P<0.001$, respectively), with SDN demonstrating significantly higher killing efficacy than BSA-linked micelles (+BSA). Overall, these results indicate that SDN displays robust cell selectivity and temperature sensitivity, outperforming the +BSA group (Figure S10).

Security evaluation of SDN

An acute toxicity evaluation of nanomicelle-encapsulated shikonin (SDN) was conducted *via* tail vein injection and multiple administrations within 24 h to assess its safety. Results indicated that out of 10 mice injected with 5.5 mg/kg of monomeric shikonin, 6 died within 24 h (Table 3), whereas only 1 mouse died after injection of SDN (L) at the same concentration. Further increasing the SDN concentration revealed that at 9 mg/kg of shikonin wrapped in SDN, only 2 mice died. Histopathological analysis of the lungs, kidneys, liver, and heart of the mice showed varying degrees of damage in the organs of those treated with monomeric shikonin. Notably, a reduction in organ damage was observed in mice treated with different concentrations of SDN compared to the monomeric shikonin group. These findings suggest that the toxicity and side effects of shikonin are significantly reduced when coated with nanomaterials, highlighting the improved safety profile of SDN (Figure 6).

In vivo efficacy of SDN in mouse subcutaneous tumor model

To confirm the anti-cancer effect of SDN *in vivo*, BT-474 cells were used to establish subcutaneous tumors for experimentation (Figure 7A). When the subcutaneous tumor mass was palpable, a shikonin drug (monomeric shikonin/+BSA/SDN) was injected at a concentration of 2 mg/kg via the tail vein. Following continuous injections for 15 days, the tumor mass was excised and weighed. Results indicated that treatment with SDN and +BSA significantly inhibited tumor growth compared to the control group (Figure 7B), leading to a notable decrease in tumor weight. Furthermore, analysis of harvested tumor tissue using immunohistochemistry revealed a significant reduction in the proportion of ki-67-positive cells after SDN treatment, consistent with the *in vitro* findings and tumor size. These results support the efficacy of SDN in suppressing tumor growth.

Discussion

Shikonin has excellent anti-tumor effect, but its slightly soluble in water greatly affects its anti-tumor effect. In our study, a high molecular support with good biocompatibility and temperature responsiveness was used to self-assemble and wrap shikonin in water by dialysis technology. The hydrophobicity of shikonin is ameliorated and the Her-2 antibody fragment is covalently linked to the surface of the carrier micelle, so that it has active targeting properties by this way. The prepared micelles were spherical in shape, with a complete core-shell structure, and the particle size was about 120 nm, which enable it enter the tumor tissue smoothly. We conducted *in vitro* studies on the prepared nanomicelles and used BSA to simulate the microenvironment *in vivo*. After mixing SDN with BSA, it could still maintain independent particle size peaks, which proved that SDN had good serum stability. We then explored the effects of various nanomicelles on breast cancer cells, and at the same concentration of shikonin, it was found that the dual-targeted micelles had the strongest killing effect on tumor cells *in vitro*.

At the same time, at different temperatures, there was no significant difference in the killing effect of shikonin monomer group on tumor cells *in vitro*. The killing effect of BSA group and SDN group at 42°C was significantly stronger than that at 37°C, because the temperature targeting property of the nanopolymer made it spontaneously gather near the cells and further inhibited cell proliferation when the local temperature increase. In addition, to verify the active targeting of the nanomicelles, we used SND to treat MCF-7 and Skbr-3 cells, respectively. The results showed that when the temperature was the same, the killing effect of SDN group and BSA group on McF-7 cells was not significantly different, while the killing effect of SDN group and BSA group on SKBR-3 cells was significantly different, and the difference was statistically significant. we also tested the toxic effect of blank nanomicelles on cells. The results fully showed that blank nanomicelles had low cytotoxic effect on cells and no cytotoxic effect

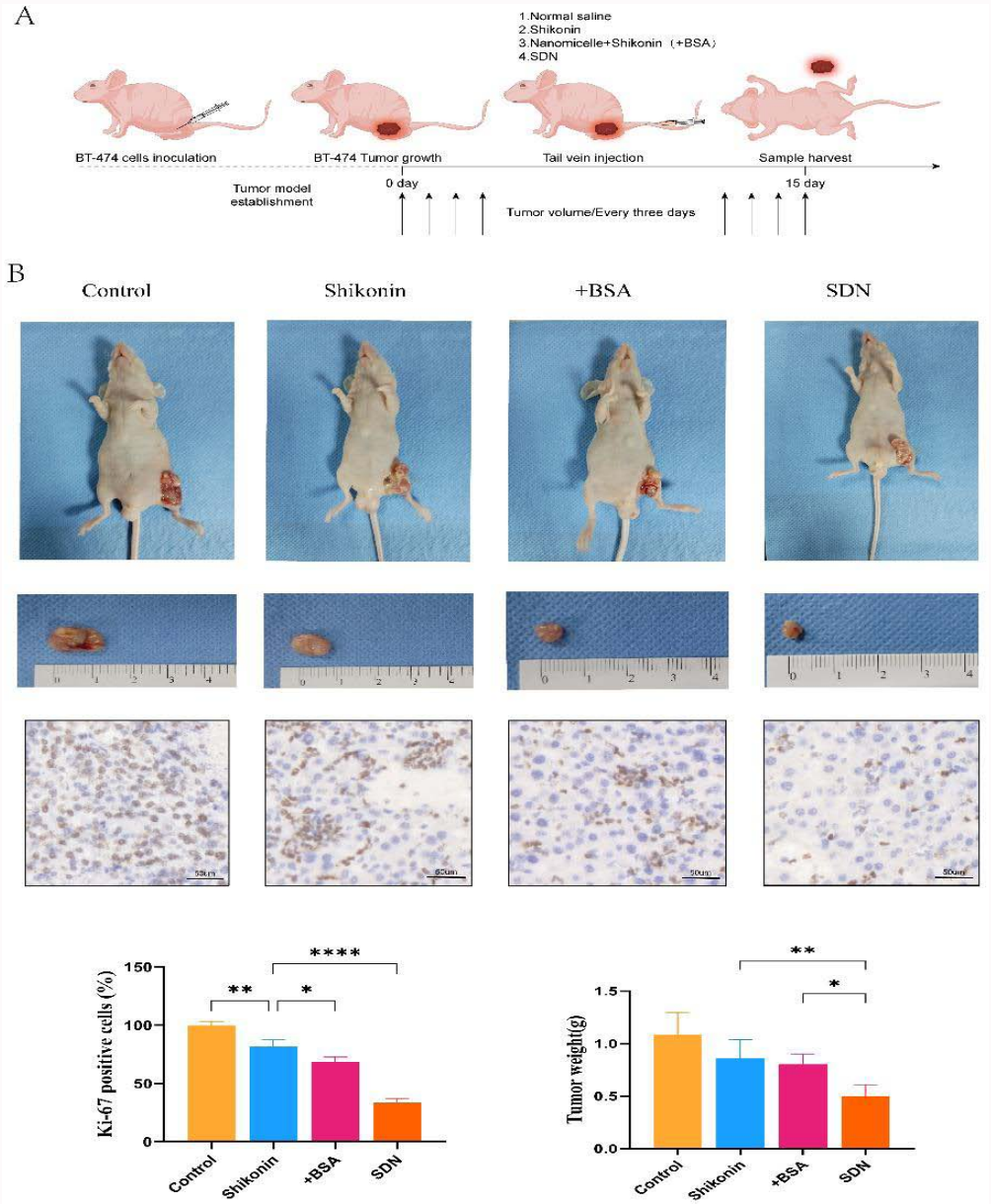

Figure 7: A) Schematic diagram of mouse subcutaneous tumor construction. B) SDN inhibits tumor growth *in vivo*, evaluates tumor weight and evaluates cell proliferation by ki-67 immunohistochemistry.

on breast cancer cells.

Afterwards, we examined the effect of the nanomicelles on the induction of programmed cell death. used flow cytometry to detect the effect of SDN on inducing apoptosis and necrosis of SKBR-3 cell. The results showed that the cell mortality of SDN group was significantly higher than that of BSA group and monomeric drug group, indicating that SDN could induce programmed death of SKBR-3 cells more effectively. At the same time, in order to verify the targeting effect of the antibody, we observed the endocytosis of cells by confocal microscopy. The results showed that the macromolecules linked by the antibody were more likely to aggregate in tumor cells, which improved the uptake of micelles by tumor cells.

Conclusion

We have successfully combined traditional Chinese medicine with modern technology by loading shikonin to the nanomicelle to prepare SDN. It has both active and passive dual targeting effects originating from the temperature sensitivity and antibody specific interaction, which enable it to increases the selectivity and lethality of polymer micelles to tumors. Through characterization detection of SDN and *in vitro* experimental verification, it can be seen that the synthesized SDN has high drug loading and encapsulation rate, complete core-shell structure and spherical shape, and good stability in serum.

CCK8 cell proliferation experiments demonstrate that Shikonin-loaded Dual targeting Nanomicelles (SDN) effectively inhibit the proliferation of Her-2 receptor-positive breast cancer cells, surpassing the efficacy of monomeric shikonin and single-targeting nanomicelles (BSA). The cytotoxicity at 42°C outweighs that at 37°C, indicating notable cell selectivity and temperature sensitivity. Findings from acute toxicity assessments reveal that SDN, at equivalent shikonin concentrations, exhibits greater safety compared to monomeric

shikonin, leading to a significant reduction in organ toxicity and side effects. In an *in vivo* mouse subcutaneous tumor model, SDN demonstrates superior inhibition of BT-474 tumor growth relative to monomeric shikonin, as supported by immunohistochemical analyses. This study's innovation lies in the development of a dual-targeted nanodrug delivery system incorporating shikonin, addressing the biocompatibility, targeting efficiency, and water solubility limitations of conventional monomeric shikonin *in vivo*. By dual-targeting tumor cells, it enhances Shikonin's efficacy against HER-2 receptor-positive breast cancer cells while mitigating organ toxicity, thereby enhancing safety. Nonetheless, the study did not delve into the specific mechanism through which shikonin inhibits breast cancer cells. The implementation of a nano drug delivery system may facilitate broader clinical utilization of traditional Chinese medicine monomeric shikonin.

Funding

This work was supported by the High-level Chinese Medicine Key Discipline Construction Project (Integrative Chinese and Western Medicine Clinic) of National Administration of TCM (zyyzdxk-2023065); Evidence-based dermatology base sponsored by State Administration of Traditional Chinese medicine.

References

1. Siegel RL, Miller KD, Jemal A. Cancer statistics, 2015. CA Cancer J Clin. 2015;65(1):5-29.
2. Li CH, Yu CH, Wang PG. An age-period-cohort analysis of female breast cancer mortality from 1990-2009 in China. Int J Equity Health. 2015:14:76.
3. Fan L, Strasser-Weippl K, Li JJ, St Louis S, Finkelstein DM, Yu KD, et al. Breast cancer in China. Lancet Oncol. 2014:15(7):e279-89.
4. Hurvitz SA, Hu YF, O'Brien N, Finn RS. Current approaches and future directions in the treatment of HER2-positive breast cancer. Cancer Treat Rev. 2013;39(3):219-29.
5. Doyle LA, Yang WD, Abruzzo LV, Krogmann T, Gao Y, Rishi AK, et al. A multidrug resistance transporter from human MCF-7 breast cancer cells. Proc Natl Acad Sci U S A. 1998;95(26):15665-70.
6. Zhang M, Chen H, GU J. Analysis of factors affecting endocrine therapy resistance in breast cancer. Oncol Lett. 2016;11(1):379-84.
7. Lu L, Qin A, Huang H, Zhou P, Zhang C, Liu N, et al. Shikonin extracted from medicinal Chinese herbs exerts anti-inflammatory effect *via* proteasome inhibition. Eur J Pharmacol. 2011;658(2/3):242-7.
8. Hashimoto S, Xu M, Masuda Y, Aiuchi T, Nakajo S, Cao J, et al. β-hydroxy isovaleryl shikonin inhibits the cell growth of various cancer cell lines and induces apoptosis in leukemia HL-60 cells through a mechanism different from those of Fas and etoposide. Biochem. 1999;125(1):17-23.
9. Li W, Liu J, Jackson K, Shi R, Zhao Y. Sensitizing the therapeutic efficacy of Taxol with Shikonin in human breast cancer cells. Plos One. 2014;9(4):e94079.
10. Wei Y, Li M, Cui S, Wang D, Zhang CY, Zen K, et al. Shikonin inhibits the proliferation of human breast cancer cells by reducing tumor-derived exosomes. Molecules. 2016;21(6):777.
11. Thakur R, Trivedi R, Rastogi N, Singh M, Mishra DP. Inhibition of STAT3, FAK and Src mediated signaling reduces cancer stem cell load, tumorigenic potential and metastasis in breast cancer. Sci Rep. 2015;5:10194.
12. Yin SY, Efferth T, Jian FY, Chen YH, Liu CI, Wang AHJ, et al. Immunogenicity of mammary tumor cells can be induced by shikonin *via* direct binding-interference with hnRNPA1. Oncotarget. 2016;7(28):43629-53.
13. Wang RB, Yin RT, Zhou W, Xu D, Li S. Shikonin and its derivatives: a patent review. Expert Opin Ther Pat. 2012;22(9):977-97.
14. Wang WJ, Dai M, Zhu CH, Zhang J, Lin L, Ding J, et al. Synthesis and biological activity of novel shikonin analogues. Bioorg Med Chem Lett. 2009;19(3):735-7.
15. Quina FH, Alonso EO, Farah JPS. Incorporation of nonionic solutes into aqueous micelles: A linear solvation free energy relationship analysis. J Phys Chem. 2002;99(30):11708-14.
16. Letchford K, Liggins R, Burt H. Solubilization of hydrophobic drugs by methoxy poly(ethylene glycol)-block-polycaprolactone diblock copolymer micelles: Theoretical and experimental data and correlations. J Pharm Sci. 2008;97(3):1179-90.
17. Li W, Nakayama M, Akimoto J, Okano T. Effect of block compositions of amphiphilic block copolymers on the physicochemical properties of polymeric micelles. Polymer. 2011;52(17):3783-90.
18. Kim S, Shi Y, Kim JY, Park K, Cheng JX. Overcoming the barriers in micellar drug delivery: Loading efficiency, in vivo stability, and micelle-cell interaction. Expert Opin Drug Deliv. 2010;7(1):49-62.
19. Haliloglu T, Bahar I, Erman B, Mattice WL. Mechanisms of the Exchange of Diblock Copolymers between Micelles at Dynamic Equilibrium. Macromolecules. 1996;29(13):4764-71.
20. Nwose EU. Whole blood viscosity assessment issues V: Prevalence in hypercreatinaemia, hyperglycaemia and hyperlipidaemia. N Am J Med Sci. 2010;2(9):403-8.
21. Batrakova E, Lee S, Li S, Venne A, Alakhov V, Kabanov A. Fundamental relationships between the composition of Pluronic block copolymers and their hypersensitization effect in MDR cancer cells. Pharm Res. 1999;16(9):1373-9.
22. Su Y, Huang N, Chen D, Zhang L, Dong X, Sun Y, et al. Successful *in vivo* hyperthermal therapy toward breast cancer by Chinese medicine Shikonin -loaded thermosensitive micelle. Int J Nanomedicine. 2017;12(1):4019-35.
23. Kang JH, Cho J, Ko YT. Investigation on the effect of nanoparticle size on the blood-brain tumor barrier permeability by *in situ* perfusion *via* internal carotid artery in mice. J Drug Target. 2019;27(1):103-10.
24. Du Y, Zhang R, Zargari A, Thai TC, Gunderson CC, Moxley KM, et al. Classification of tumor epithelium and stroma by exploiting image features learned by deep convolutional neural networks. Ann Biomed Eng. 2018;46 (12):1988-99.
25. Othman MS, Obeidat ST, Al-Bagawi AH, Fareid MA, Fehaid A, Moneim AEA. Green-synthetized selenium nanoparticles using berberine as a promising anticancer agent. J Integr Med. 2022;20(1):65-72.
26. Liang P, Huang X, Wang Y, Chen D, Ou C, Zhang Q, et al. Tumor-microenvironment-responsive nanoconjugate for synergistic antivascular activity and phototherapy. ACS Nano. 2018;12(11):11446-57.
27. Seven PT, Seven I, Karakus S, Mutlu SI, Kaya SO, Arkali G, et al. The in-vivo assessment of Turkish propolis and its nano form on testicular damage induced by cisplatin. J Integr Med. 2021;19(5):451-9.
28. Gou H, Huang RC, Zhang FL, Su YH. Design of dual targeting immunomicelles loaded with bufalin and study of their anti-tumor effect on liver cancer. J Integr Med. 2021;19(5):408-17.
29. Maeda H. The Enhanced Permeability and Retention (EPR) effect in tumor vasculature: The key role of tumor-selective macromolecular drug targeting. Adv Enzyme Regul. 2001;41(1):189-207.
30. Zheng C, Qiu LY, Yao XP, Zhu KJ. Novel micelles from graft polyphosphazenes as potential anti-cancer drug delivery systems: Drug encapsulation and in vitro evaluation. Int J Pharm. 2009;373(1-2):133-40.